Korean J. Chem. Eng., **29**(1), 95-102 (2012)
DOI: 10.1007/s11814-011-0137-y

Arsenic adsorption on goethite nanoparticles produced through hydrazine sulfate assisted synthesis method

Malay Kumar Ghosh†,‡, Gérrard Eddy Jai Poinern, Touma B. Issa, and Pritam Singh

School of Chemical and Mathematical Sciences, Murdoch University, WA 6150, Australia
(*Received 25 January 2011 • accepted 17 May 2011*)

Abstract−Goethite nanoparticles synthesized using hydrazine sulfate as a modifying agent were evaluated for As(V) adsorption capacity. The nanoparticles were characterized for their morphological and structural features. The precipitated goethite particles were spherical with particle size of less than 10 nm. Batch adsorption study was carried out systematically varying parameters such as pH, contact time, initial As(V) concentration and adsorbent doses. The Langmuir isotherm represented the equilibrium data well and the estimated monolayer adsorption capacity at ambient temperature was 76 mg/g, which is significantly higher than most of the adsorbents reported in the literature. Adsorption kinetic data were better represented by the pseudo-second order kinetic model. Intra-particle diffusion played a significant role in the rate controlling process in the initial hour. Desorption study showed that the loaded adsorbent could be regenerated when treated with dilute sodium hydroxide solution of pH 13.

Key words: Arsenic, Goethite, Adsorption, Isotherms, Nanoparticles

INTRODUCTION

Arsenic is a highly toxic and carcinogenic element. Contamination of ground water with this element from both natural and anthropogenic sources has become a great global concern. Arsenic is a constituent of more than 245 minerals and mainly associated with sulfide minerals - smelting of which emits more than 60,000 tons annually [1]. WHO [2] recommends a maximum arsenic concentration level of 0.01 mg/L in drinking water, although many countries still follow the previous concentration limit of 0.05 mg/L. To bring the contamination level down to an acceptable limit, several techniques have been followed which are broadly based on oxidation-precipitation, coagulation-precipitation, adsorption-ion exchange, membrane processes etc. [3]. However, the most sought-after technique has been adsorption due to its simple operational procedure and cost.

Phenomenal development in the field of nanotechnology towards the end of 20th century has widened the scope of nanoadsorbents for toxic metal ions and anions. Different types of nanomaterials have been used for the removal of arsenic from contaminated water, such as titanium dioxide [4], iron oxides [5,6], zero valent iron [7] and modified zero valent iron particles [8]. Iron oxide nanoparticles are able to bind arsenic 5 to 10 times more effectively than micron-sized particles [9].

Nanophase iron oxide/hydroxide compounds are important constituents of soils and sediments and possess high sorption capacities for metal ions and anions such as those of arsenic, chromium, lead, mercury and selenium. Waychunas et al. [10] discussed the structures and reactivity of goethite, akaganeite, hematite, ferrihydrite and schwertmannite nanoparticles in natural systems.

Goethite (α-FeOOH) is the most widespread crystalline iron oxide in soils and sediments. Several studies have been carried out on arsenic sorption onto goethite, especially related to the As(V) sorption [11-13]. Matis et al. [13] used a novel process where arsenic was removed from dilute aqueous solutions by sorption onto synthetic goethite then subsequent flotation as an effective solid/liquid separation method. The investigation by Bowell [14] showed that the sorption of As(III) as well as As(V) was higher on natural goethite than that on natural magnetite and the adsorption was higher for As(V) than for As(III). The maximum sorption occurred at neutral pH.

To understand the molecular structure of ions retained on the mineral surface, Fendorf et al. [15] studied the local coordination state of arsenate and chromate on the surface of goethite using extended X-ray absorption fine structure (EXAFS) spectroscopy. It was reported that three different surface complexes existed on goethite surface: a monodentate complex, a bidentate-binuclear complex and bidentate-mononuclear complex. At low surface coverage monodentate complex was favored while at higher surface coverage bidentate was favored.

The objective of the present study was to precipitate nanogoethite assisted by hydrazine sulfate additive and to study its potential application for the removal of arsenic from aqueous solution. The strong reducing power, monodented ligand property, ability to scavenge oxygen, and formation of moisture and nitrogen as decomposition by-products are the key advantages to consider hydrazine as a potential additive, in comparison to other alternates such as urea and glycine. The detailed characterization of goethite nanoparticles was carried out using different instrumental techniques, and the equilibrium and kinetic data from the batch adsorption studies were analyzed through different models to understand the adsorption mech-

†To whom correspondence should be addressed.
E-mail: m_k_ghosh@yahoo.com
‡Present address: Institute of Minerals and Materials Technology, Bhubaneswar 751013, India.

anism of As(V) on the goethite sample.

MATERIALS AND METHODS

1. Synthesis of Adsorbent

The goethite nanoparticles were prepared adding 7.5 g of hydrazine sulfate ($N_2H_6SO_4$) to 100 mL ferric nitrate solution (1 M) with continuous stirring until a clear solution of yellowish brown was obtained. The solution was heated at 90 °C for one hour in a closed reactor and then allowed to cool inside. The solution pH was then adjusted to about 3.0 by adding 1.0 M NaOH solution under constant stirring. The precipitate was filtered and washed with doubly-distilled water thoroughly till free of sulfate and nitrate and then dried in an air oven at 100 °C for 24 hours.

2. Characterization of Adsorbent

The X-ray diffraction (XRD) pattern of the prepared goethite sample was taken in a Philips Analytical PW-1830 powder diffractometer using Co Kα radiation source at a scan speed of 1.2°/min.

For transmission electron microscopy (TEM) a small amount of the goethite sample was sonicated in ethyl alcohol under low power for dispersion. The suspension was then deposited onto a carbon coated copper grid and dried for about 24 h. TEM study was carried out at 80 kV with PHILIPS CM-100 Electron Microscope.

To carry out Fourier transform infrared spectroscopic (FTIR) study, a small amount of representative sample was mixed with spectroscopic grade KBr and then pelletized. Spectrum was recorded with a DTGS-KBr detector in Thermo Scientific Nicolet 6700 FTIR (USA) model from 400 cm^{-1} to 4,000 cm^{-1} with a resolution of 4.0 cm^{-1}.

The morphological features of the goethite sample were studied with a high resolution field emission scanning electron microscope (Zeiss 1555 VP-FESEM) at 3 kV with 30 μm aperture under 1×10^{-10} Torr pressure.

3. Adsorption Studies

First, a standard stock solution of 1,000 mg/L As(V) was prepared by dissolving 8.26 g of sodium arsenate in 2 L of MilliQ® ultra-pure water. An aliquot of the standard As (1,000 mg/L) solution was taken and diluted to required concentration and pH. Solution pH was adjusted with dilute HNO_3 and/or NaOH solution. From this solution 100 mL was taken in a dried 250 mL Schott® bottle to which 0.1 g adsorbent was added (except where adsorbent dose was varied). Bottles were tightly closed and placed in the Perth Scientific® shaker water bath set at 75 rpm shaking speed and 298 K temperature. Adsorption experiments continued for a predetermined time after which about 50 mL supernatant liquor was filtered twice using 0.22 μm Millipore syringe filter unit. Arsenic analysis was carried out using Varian ICP-AES (Model: Vista AX CCD Simultaneous ICP-AES) located in Murdoch University's Marine and Freshwater Research Laboratory which is NATA (National Association of Testing Authorities, Australia) accredited.

4. Desorption Studies

For desorption experiments, first As(V) was adsorbed on the goethite adsorbent under the following conditions: 50 mg/L As(V) solution, pH 3.0, 1 g/L adsorbent dose and agitation time 4 h. After adsorption, suspensions were filtered, washed and air dried. Then 50 mL solution of different pH was added to the 0.05 g loaded adsorbent. The samples were then shaken for 4 h and filtered. As(V) concentration in the filtrate was analyzed, and desorption efficiency was calculated.

RESULTS AND DISCUSSION

1. Characterization of the Synthesized Goethite

The surface area of the synthesized sample was measured using Quantasorb 1750 after degassing, and the specific surface area was found to be 167.8 m^2/g.

The XRD pattern of the synthesized goethite sample is shown in Fig. 1. The spectrum of the goethite sample contains all the major peaks referring to JCPDS card No. 17-0536, thus indicating the formation of α-FeOOH. The main (hkl) indices of goethite like (020), (110), (120), (130), (021), (111), (121), (140), (131), (041), (211) and (221) are clearly indicated in the pattern. The peaks are slightly broad, indicating a smaller crystal size.

FESEM image shown in Fig. 2 reveals spherical clusters but mostly agglomerated. The TEM micrograph shows clearer view about the morphology and size of individual particles because of sonication carried out before preparing sample for TEM. Fig. 3 shows that the particles are extremely small (<10 nm) and mostly uniform in size.

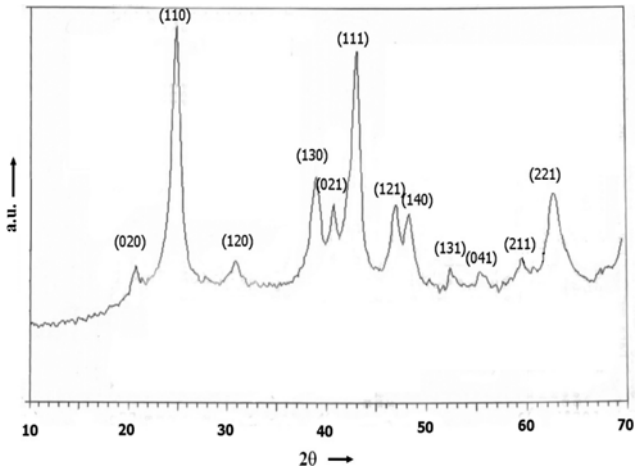

Fig. 1. XRD pattern of goethite sample.

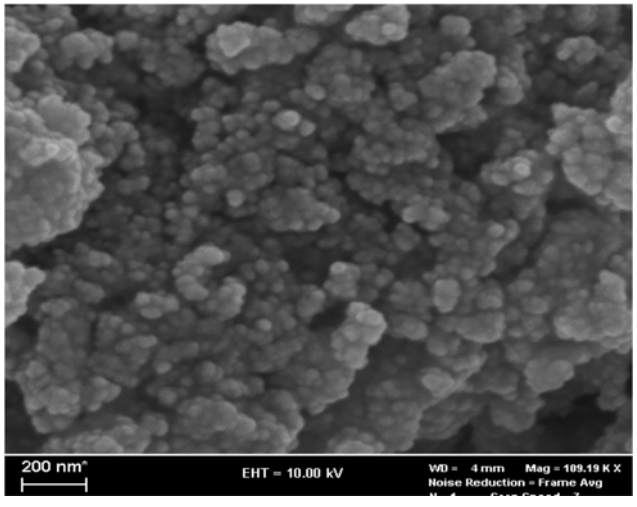

Fig. 2. FESEM micrograph of the synthesized nano-goethite.

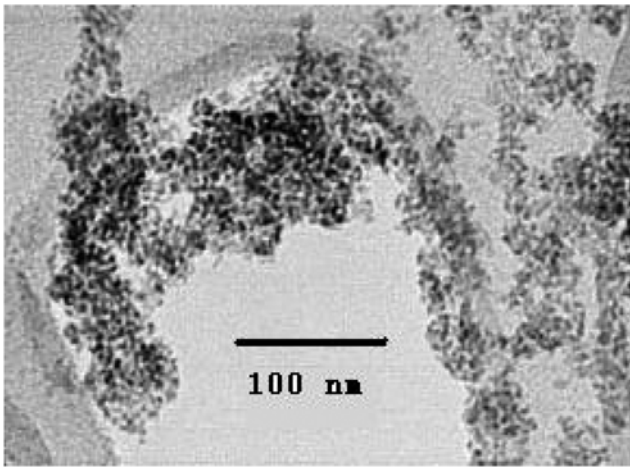

Fig. 3. TEM image of the synthesized nano-goethite.

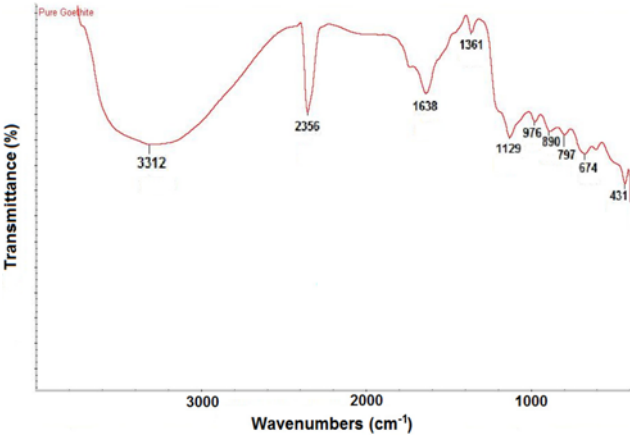

Fig. 4. FTIR spectra of goethite sample.

FTIR spectrum of the nanogoethite sample is shown in Fig. 4. The very broad IR band at 3,312 cm^{-1} can be attributed to the stretching vibration of surface H_2O molecules or the hydrogen bonded surface OH groups. The sharp and intense band at 1 638 cm^{-1} is typical for the bending vibration of OH group. The band at 1,129 cm^{-1} can be assigned to specifically adsorbed SO_4 groups [16]. The characteristic sharp bands at 797 cm^{-1} and 890 cm^{-1} can be assigned to the Fe-O-OH bending vibration in α-FeOOH. The 674 cm^{-1} and 431 cm^{-1} bands are ascribed to Fe-O stretching vibrations of goethite lattice [17]. These bands are affected by the shape of the goethite particles [17,18]. Strong bands at 2,356 cm^{-1} and 1,361 cm^{-1} can be assigned to the presence of CO_3^{-2} due to the contamination by atmospheric CO_2 [19].

2. Adsorption Studies

2-1. Effect of pH

Fig. 5 shows the effect of pH (in the range 2-10) on adsorption efficiency of goethite. It is observed that with increase in pH beyond 3 As(V) adsorption percentage decreases significantly. As(V) predominantly exists as $H_2AsO_4^-$ and $HAsO_4^{2-}$ in the pH range of 2.7 to 11.5 [20]. Acidic solution provides sufficient protonated sites to the adsorbent. This results in a net positive surface charged substrate which will attract negatively charged oxyanions.

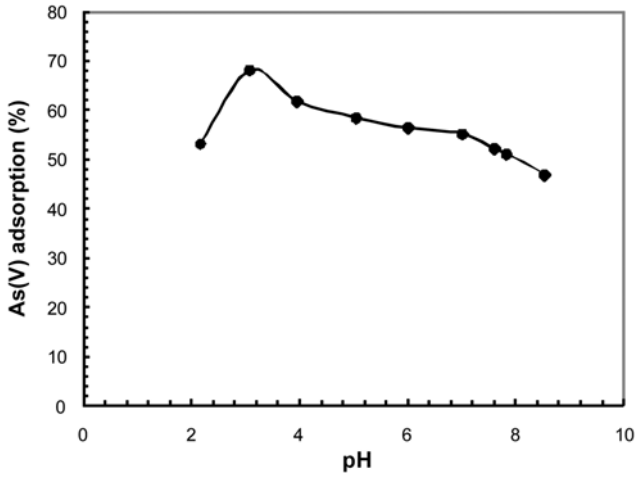

Fig. 5. Effect of pH on extent of adsorption [Conditions: Initial [As (V)] 50 mg/L, adsorbent dose 1 g/L, 298 K, Time 2.5 h].

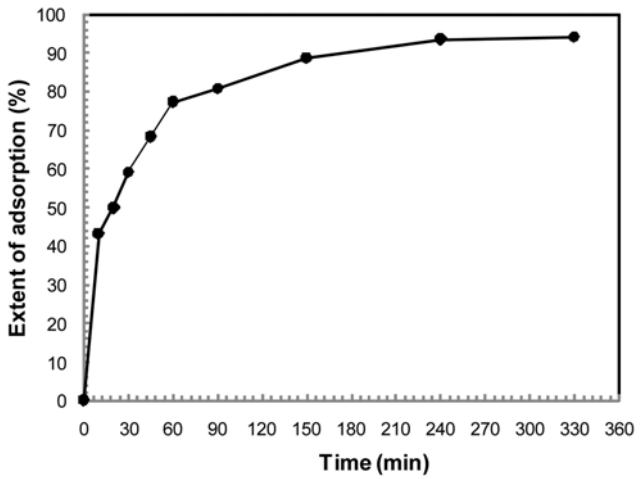

Fig. 6. Effect of time on percent adsorption [Conditions: pH 3.0, initial [As(V)] 50 mg/L, 298 K, adsorbent dose 1 g/L].

The protonation/deprotonation of surface hydroxyl groups can be represented by the following reactions:

$$\equiv SOH + H^+ \leftrightarrow \equiv SOH_2^+$$

$$\equiv SOH \leftrightarrow SO^- + H^+$$

Where $\equiv SOH$, $\equiv SOH_2^+$ and $\equiv SO^-$ are uncharged, positively charged and negatively charged surface groups, respectively.

With increase in pH the number of negatively charged sites increases and the number of positively charged sites decreases. A negatively charged site does not favor adsorption due to electrostatic repulsion. Below pH 2.7 As(V) predominantly exists in the form H_3AsO_4 which cannot be adsorbed under electrostatic attraction due to charge neutrality.

2-2. Adsorption Kinetics

Fig. 6 shows the adsorption efficiency as a function of time. Uptake of arsenic by goethite takes place in two distinct stages - an initial fast adsorption stage (up to 60 min) followed by a slow step. Adsorption efficiency of 77% is achieved within contact time of 1 hour and finally 94% after 5.5 hours. It is also observed that equilibrium

is achieved in 4 h, hence all further experiments were carried out keeping contact time 4 h.

To investigate the mechanism of adsorption and determine the rate constants, three widely used kinetic models were tested - pseudo-first order, pseudo-second order and intra-particle diffusion (IPD).

The Lagergren pseudo-first order rate law [21] can be expressed in the linear form as:

$$\log(q_e - q_t) = \log q_e - \frac{k_1}{2.303}t \quad (1)$$

And pseudo-second order rate equation [22] in the linear form is

$$\frac{t}{q_t} = \frac{1}{k_2 q_e^2} + \frac{1}{q_e}t \quad (2)$$

Where, q_e (mg/g) and q_t (mg/g) are adsorbate concentration at equilibrium and at time t respectively and k_1 (/min) and k_2 (g/min·mg) are the pseudo-first order and pseudo-second order adsorption rate constants, respectively. Time variant adsorption data were plotted as per Eqs. (1) and (2) and are shown in Figs. 7 and 8, respectively.

Different rate constants and R^2 values determined from the linear plots are given in Table 1. Although both the kinetic equations result in linear plots with R^2 values of more than 0.99, the pseudo-second order plot represents the kinetic data better because the calculated equilibrium adsorption value matches more closely with the experimentally obtained value.

In a sorption system when there is a possibility of intra-particle diffusion being the rate limiting step, the intra-particle diffusion (IPD) model developed by Weber and Morriss [23] is applied. The IPD model is expressed as:

$$q_t = k_p t^{1/2} + C \quad (3)$$

where k_p is the IPD rate constant (mg/g·min$^{1/2}$·g), and C is the intercept which is related to boundary layer thickness. According to this model, if intra-particle diffusion is involved in the adsorption system, then the q_t versus the $t^{1/2}$ plot should be linear; and if the line passes through the origin, then intra-particle diffusion is the only rate-controlling step.

However, if the data exhibit multilinear plots, then two or more steps may influence the adsorption process. The IPD model fitted to kinetic data results in a multilinear plot (Fig. 9). The first stage (line not shown for clarity) is mass transfer of adsorbate ions from the bulk phase to the adsorbent surface. The second stage shown by the dotted

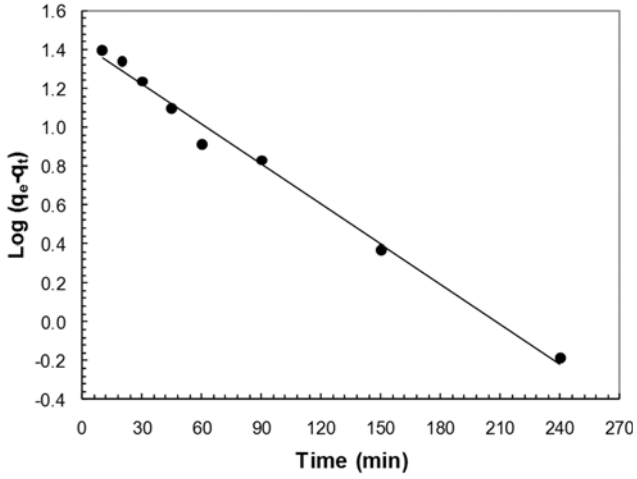

Fig. 7. Lagergren pseudo-first order plot [Conditions: pH 3.0, initial [As(V)] 50 mg/L, 298 K, adsorbent dose 1 g/L].

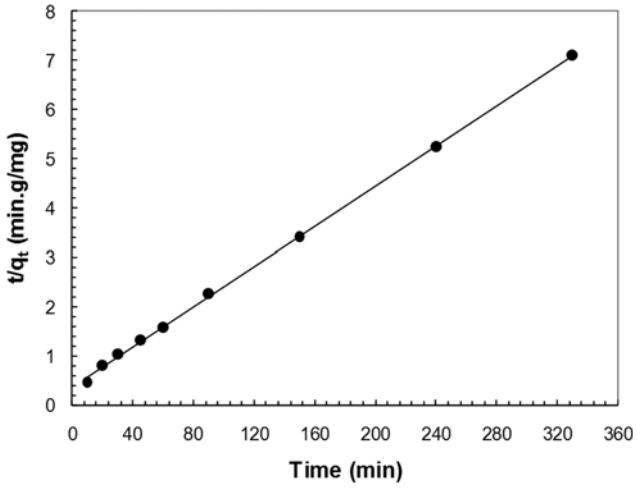

Fig. 8. Pseudo-second order plot [Conditions: pH 3.0, initial [As (V)] 50 mg/L, 298 K, adsorbent dose 1 g/L].

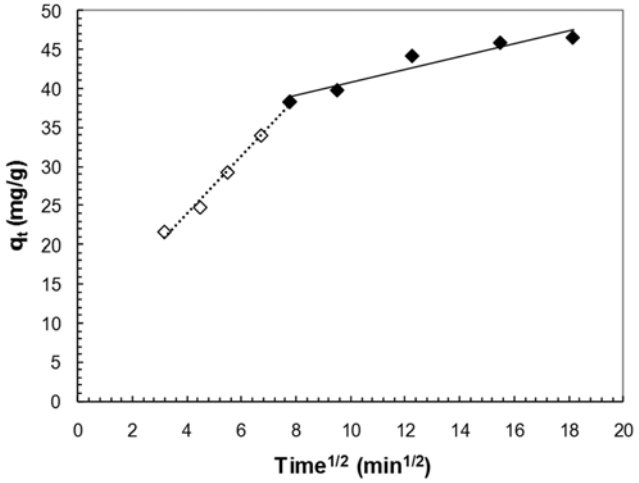

Fig. 9. Intra-particle diffusion plot [Conditions: pH 3.0, initial [As (V)] 50 mg/L, 298 K, adsorbent dose 1 g/L].

Table 1. Rate constants and correlation coefficients for the studied models

$q_{e,exp}$ (mg/g)	Pseudo-first order			Pseudo-second order			Intra-particle diffusion		
	$q_{e,cal}$ (mg/g)	k_1 (/min)	R^2	$q_{e,cal}$ (mg/g)	k_2 (g/mg·min)	R^2	k_p (mg/g·min$^{1/2}$)	C (mg/g)	R^2
46.44	26.68	0.016	0.992	49.02	1.12×10^{-3}	0.999	3.72	9.047	0.99

line is the intra-particle diffusion on the goethite for which the calculated rate constants and intercept values are given in Table 1.

2-3. Adsorption Isotherms

The adsorption isotherms express the relationship between the equilibrium concentrations of adsorbate in the aqueous phase and on the solid surface at constant temperature. Equilibrium data were obtained varying initial concentration from 5 to 100 mg/L at pH 3.0, adsorbent dose 1 g/L and 4 h contact time. Maximum adsorption achieved under the above conditions was 72.4 mg As(V)/g of goethite at initial As(V) concentration of 100 mg/L Two widely used isotherms, Freundlich and Langmuir, were tested with equilibrium data. The Langmuir model is based on the assumption of monolayer coverage and that structure of adsorbent is homogeneous where all sorption sites are identical and energetically equivalent while the basis of Freundlich model is physicochemical adsorption on heterogeneous surfaces. The linear forms of the two models are:

$$\text{Langmuir} \quad \frac{C_e}{q_e} = \frac{C_e}{q_{max}} + \frac{1}{q_{max} \cdot K_L} \tag{4}$$

$$\text{Freundlich:} \quad \ln q_e = \ln K_F + \frac{1}{n} \ln C_e \tag{5}$$

Where, q_e (mg/g) and C_e (mg/L) are equilibrium As(V) concentration on the adsorbent and in solution, respectively, q_{max} (mg/g) is the monolayer adsorption capacity, K_L (L/mg) is Langmuir adsorption constant related to the free energy of adsorption. K_F (mg/g)(mg/L)$^{-1/n}$ and n (dimensionless) are Freundlich adsorption isotherm constants being indicative of extent of adsorption and intensity of adsorption, respectively.

A linear plot (Fig. 10) of the experimental data as per Langmuir isotherm equation has R^2 value of 0.999, indicating a well fit model.

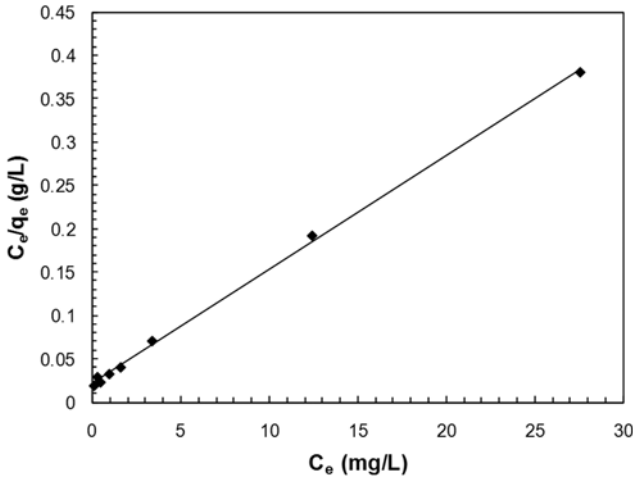

Fig. 10. Langmuir isotherm plot of adsorption data [Conditions: pH 3.0, contact time 4 h, 298 K, adsorbent dose 1 g/L].

Table 2. Adsorption isotherm parameters

Langmuir isotherm		Freundlich isotherm	
q_{max} (mg/g)	76.34	K_F(mg/g)·(mg/L)$^{-1/n}$	22.03
K_L (L/mg)	0.6	n	2.13
R^2	0.999	R^2	0.891

But when adsorption data are plotted as per Freundlich isotherm, it results in a poor fit with an R^2 value of 0.89. Similar observations with other adsorbents are well reported in the literature [24,25]. Different constants calculated from the slopes and intercepts for both the models are given in Table 2.

The isotherm shape of the Langmuir plot is used to predict the favorability of an adsorption system. The favorability of adsorption can be expressed in terms of a dimensionless constant separation factor or equilibrium parameter R_L [26] expressed by Eq.(6).

$$R_L = \frac{1}{1 + K_L C_0} \tag{6}$$

Where, K_L is the Langmuir constant (L/mg) and C_0 is the initial As(V) concentration (mg/L). The value of R_L indicates the shape of the isotherm, such as,

R_L>1 unfavorable
R_L=1 linear
R_L<1 & >0 favorable
R_L=0 irreversible

The R_L values estimated at different concentrations vary from 0.25 (at 5 mg/L) to 0.01 (at 100 mg/L), which indicates that adsorption is favorable in the studied concentration range. The favorability is higher at higher initial concentration.

2-4. Effect of Adsorbent Dose

To study the effect of adsorbent dose on percent arsenic adsorption the dose was varied from 1 to 8 g/L keeping other parameters constant: pH 3.0, initial arsenic concentration 50 mg/L, contact time 4 h and temperature 298 K. Fig. 11 shows the effect of adsorbent dose on the percent arsenic adsorption.

It can be observed in Fig. 11 that with the increase in adsorbent dose, the percent adsorption of arsenic initially increases rapidly followed by a slow increase. This might be related to an increase in active sites with increase in the amount of adsorbent. At adsorbent dose of >4 g/L there is not much increase in the adsorption efficiency. Beyond 6 g/L of adsorbent dose the arsenic removal efficiency reached a plateau.

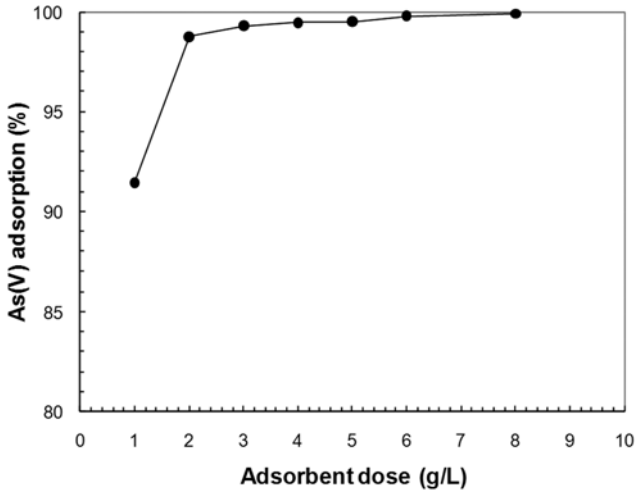

Fig. 11. As(V) adsorption at different adsorbent doses [Conditions: pH 3.0, contact time 4 h, 298 K, initial [As(V)] 50 mg/L].

According to surface sites heterogeneity model, with increase in adsorbent dose, binding ability of the surface for an ion increases due to increase in surface hydroxyl group [27]. This can be illustrated by a separation factor K_D which can be expressed as:

$$K_D = \frac{C_s}{C_e} \quad (7)$$

Where, C_s and C_e are equilibrium concentrations of As (V) at solid surface (mg/g) and in solution (mg/L), respectively. From Fig. 12 it can be observed that the K_D value increases with the increase in adsorbent dose, which implies that surface of goethite is heterogeneous. At higher adsorbent concentration of >6 g/L K_D value does not change, suggesting that the available sites for adsorbing 50 mg/L As(V) are well in excess, hence no change is obvious.

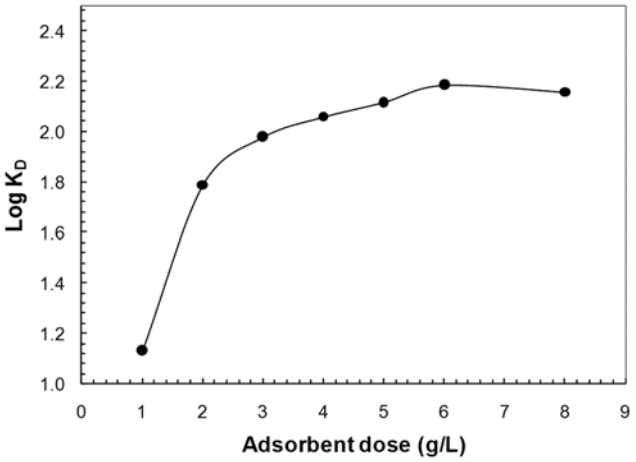

Fig. 12. Log K_D value as a function of adsorbent dose [Conditions: pH 3.0, contact time 4 h, 298 K, initial [As(V)] 50 mg/L].

3. Desorption Study

The potential application of an adsorbent depends not only on its adsorption capacity but also on its regeneration ability. Desorption studies help to indicate regeneration ability of the adsorbent. Several studies have indicated that once adsorbed on goethite surface, arsenate is not easily desorbed or removed, unless pH conditions severely change. From the experimental studies on arsenate adsorption/desorption kinetics in goethite, O'Reilly et al. [28] showed that the surface complex is very stable at pH 4 and 6 for extended time. Results obtained in the present investigation (Fig. 13) show

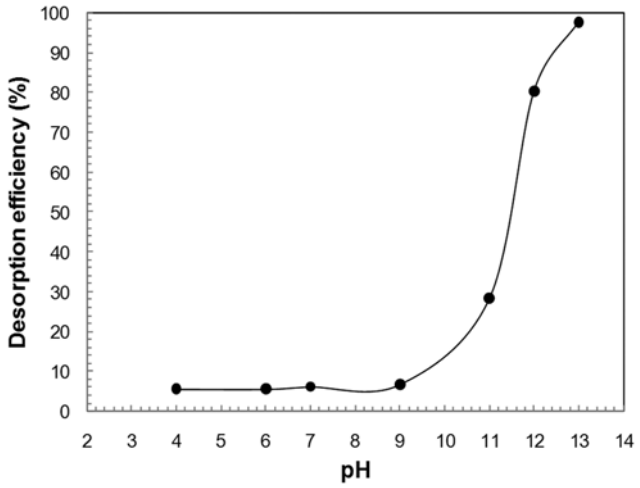

Fig. 13. Percent desorption of As(V) from loaded adsorbent at different pH [Conditions: Contact time 4 h, 298 K, adsorbent dose 1 g/L].

Table 3. Monolayer As(V) adsorption capacity of different materials reported in the literature

Adsorbent	Adsorption capacity (mg/g)	Experimental conditions		Reference
		pH	Concentration (mg/L)	
Goethite	76.3	3	5-100	This work
Maghemite				
CM	16.7			
SM	25	3	1-11*	[6]
MM	50			
Activated alumina	16.1	4	1-25	[20]
	20.6	7	1-25	
Fe-Ti oxide	14.6	7	n.a.	[29]
Akaganite (βFeOOH)	120	7.5	5-20	[30]
Basic yttrium carbonate	352.5*-427*	7.5-9	750-4500*	[31]
Maghemite	4.64	7	1-4	[32]
Calcined bauxite ore	1.78	7	n.a.	[33]
Synthetic zeolite				
H24	35.8	6.5	10-150	[34]
H90	34.8	3.2	10-150	
Carbon black				
CB-C	50.14	5	5-200	[35]
CB-S	62.52	4	5-200	

*Converted from other unit
n.a. Not available

that desorption efficiency of As-loaded goethite is very low up to solution pH 9, beyond which it enhances rapidly. At pH 13 nearly 98% desorption occurs. Similar observations were reported by Tripathy and Raichur [20].

4. Comparative Evaluation of Different Adsorbents for As(V) Removal

Monolayer adsorption capacity of an adsorbent can be estimated from the Langmuir isotherm, which indicates the possible maximum adsorption capacity in a range of arsenic concentration. It is worthwhile to compare the monolayer adsorption capacity obtained in the present investigation vis-à-vis values reported for other adsorbents in the literature (Table 3). It is evident from Table 3 that the monolayer adsorption capacity of goethite synthesized in the present investigation has comparatively much higher value than obtained with most of the other adsorbents.

Another important aspect is the possible secondary pollution during the use of an adsorbent for remediation. In the present investigation although goethite has been found to have active surface for adsorption, but dissolution of iron from the adsorbent during sorption process was negligibly small. Iron contamination after adsorption was found to be less than 0.1 mg/L in the pH range (3 to 10), which is below the WHO limit of 0.3 mg/L. However, at pH 2.0 about 2 mg/L iron contamination was observed.

CONCLUSIONS

The present study clearly demonstrated that nanoparticulate goethite obtained thorough hydrazine sulfate assisted wet-chemical synthesis method is an effective adsorbent for the removal of As(V) from aqueous solution. The adopted synthesis method generated mostly spherical particles of uniform size with surface area of 168 m^2/g. Maximum adsorption occurred at pH 3.0. The adsorption data fitted well to the Langmuir isotherm equation supporting that adsorption was monolayer. The maximum adsorption capacity (72.4 mg/g) obtained experimentally (at 100 mg/L initial arsenic concentration) matched closely with the monolayer adsorption capacity (76.3 mg/g) calculated from Langmuir isotherm. An adsorbent dose of 6 g/L is adequate for removing more than 99% As(V) from a solution containing 50 mg/L As(V). The experimental kinetic data were better represented by the pseudo-second order model. The rate controlling mechanism during the first one hour might be a combination of adsorption followed by intra-particle diffusion. It is also evident that As-loaded adsorbent can be easily regenerated by treating with dilute alkaline solution of pH 13.0.

ACKNOWLEDGEMENTS

The work was supported through the Australia-India Strategic Research Fund. The authors wish to thank Dale Parsonage of the School of Chemical and Mathematical Sciences, Murdoch University for his assistance in some parts of this work. One of the authors (MKG) thankfully acknowledges the Visiting Research Fellowship offered by Murdoch University.

NOMENCLATURE

C : intercept in the Intra-particle diffusion model [mg/g]
C_0 : initial adsorbate concentration [mg/ L]
C_e : equilibrium adsorbate concentration in solution [mg/L]
C_s : equilibrium adsorbate concentration on the adsorbent surface [mg/g]
k_1 : pseudo-first order rate constant [/min]
k_2 : pseudo-second order rate constant [g/mg·min]
K_D : separation factor [dimensionless]
K_F : Freundlich isotherm parameter [mg/g] $[mg/L]^{-1/n}$
K_L : Langmuir isotherm constant related to free energy of adsorption [L/mg]
k_P : intra-particle diffusion rate constant $[mg/g \cdot min^{1/2}]$
n : dimensionless exponent of Freundlich equation
q_e : adsorption capacity at equilibrium [mg/g]
$q_{e,cal}$: calculated equilibrium adsorption capacity [mg/g]
$q_{e,exp}$: experimentally obtained equilibrium adsorption capacity [mg/g]
q_{max} : maximum monolayer adsorption capacity [mg/g]
q_t : amount of adsorbate per unit mass of adsorbent at any time t [mg/g]
R_L : dimensionless constant separation factor

REFERENCES

1. M. Bissen and F. H. Frimemel, *Acta Hydroch. Hydrob.*, **30**(1), 9 (2003).
2. WHO (World Health Organisation) Guidelines for drinking water quality (1993).
3. D. Mohan and C. U. Pittman, *J. Hazard. Mater.*, **142**, 1 (2007).
4. M. E. Pena, G. P. Korfiatis, M. Patel, L. Lippincott and X. Meng, *Water Res.*, **39**, 2327 (2005).
5. J. T. Mayo, C. Yavuz, S. Yean, L. Cong, H. Shipley, W. Yu, J. Falkner, A. Kan, M. Tomson and V. L. Colvin, *Sci. Technol. Adv. Mat.*, **8**, 71 (2007).
6. T. Tuutijärvi, J. Lu, M. Sillanpää and G. Chen, *J. Hazard. Mater.*, **166**, 1415 (2009).
7. S. R. Kanel, J.-M. Greneche and H. Choi, *Environ. Sci. Technol.*, **40**, 2045 (2006).
8. G. Jegadeesan, K. Mondal and S. B. Lalvani, *Environ. Progr.*, **24**, 289 (2005).
9. S. Yean, L. Cong, C. T. Yavuz, J. T. Mayo, W. W. Yu, A. T. Kan, V. L. Calvin and M. B. Tomson, *J. Mater. Res.*, **20**(12), 3255 (2005).
10. G. A. Waychunas, C. S. Kim and J. F. Banfield, *J. Nanopart. Res.*, **7**, 409 (2005).
11. P. R. Grossl and D. L. Sparks, *Geoderma*, **67**, 87 (1995).
12. B. A. Manning, S. E. Fendorf and S. Goldberg, *Environ. Sci. Technol.*, **32**, 2383 (1998).
13. K. A. Matis, A. I. Zouboulis, F. B. Malamas, M. D. R. Afonso and M. J. Hudson, *Environ. Pollut.*, **97**, 239 (1997).
14. R. J. Bowell, *Appl. Geochem.*, **9**, 279 (1994).
15. S. Fendorf, M. J. Eick, P. Grossl and D. L. Sparks, *Environ. Sci. Technol.*, **31**(2), 315 (1997).
16. S. Music, A. Sanc, S. Popovic, K. Nomura and T. Sawada, *Croat. Chem. Acta*, **73**(2), 541 (2000).
17. K. M. Parida and J. Das, *J. Colloid Interface Sci.*, **178**, 586 (1996).
18. H. D. Ruan, R. I. Frost, J. T. Kloprogge and L. Duong, *Spectrochim. Acta A*, **58**, 967 (2002).
19. M. Ristic, E. De Grave, S. Music, S. Popovic and Z. Orehovec, *J.*

Molecular Structure, **834-836**, 454 (2007).
20. S. S. Tripathy and A. M. Raichur, *Chem. Eng. J.*, **138**, 179 (2008).
21. S. Lagergren, *Kungliga Svenska Vetenskapsakademiens Handlingar*, **24**, 1 (1898).
22. G. McKay and Y. S. Ho, *Process Biochem.*, **34**, 451 (1999).
23. W. J. J. Weber and J. C. Morris, *J. Sanit. Eng. Div. Am. Soc. Civil Engineers*, **89**, 31 (1963).
24. H. S. Altundogan, S. Altundogan, F. Tumen and M. Bildik, *Waste Manage.*, **20**, 761 (2000).
25. M. A. Anderson, J. F. Ferguson and J. Gavis, *J. Colloid Interface Sci.*, **54**, 391 (1976).
26. K. R. Hall, L. C. Eagleton, A. Acrivos and T. Vermeulen, *Ind. Eng. Chem. Fundam.*, **5**, 212 (1966).
27. L. Sigg, Aquatic Surface Chemistry: Chemical Processes at the Particle-Water Interface. In: Stum W. (Ed.), John Wiley and Sons, New York (1987).
28. S. E. O'Reilly, D. G. Strawn and D. L. Sparks, *Soil Sci. Soc. Am. J.*, **65**, 67 (2001).
29. K. Gupta, S. Saha and U. C. Ghosh, *J. Nanopart. Res.*, **20**, 1361 (2008).
30. P. M. Solozhenkin, E. A. Deliyanni, V. N. Bakoyannakis, A. I. Zouboulis and K. A. Matis, *J. Min. Sci.*, **39**(3), 287 (2003).
31. S. A. Wasay, M. J. Haron, A. Uchiumi and S. Tokunaga, *Water Res.*, **30**(5), 1143 (1996).
32. H. Park, N. V. Myung, H. Jung and H. Choi, *J. Nanopart. Res.*, **11**, 1981 (2009).
33. D. Mohapatra, D. Mishra and K. H. Park, *J. Environ. Sci.*, **20**, 683 (2008).
34. P. Chutia, S. Kato, T. Kojima and S. Satokawa, *J. Hazard. Mater.*, **162**, 440 (2009).
35. D. Borah, S. Satokawa, S. Kato and T. Kojima, *J. Colloid Interface Sci.*, **319**, 53 (2008).